A Novel Twofold Approach to Enhance NB-IoT MAC Procedure in NTN

Carla Amatetti, *Member, IEEE*, Madyan Alsenwi, *Member, IEEE*, Houcine Chougrani, Alessandro Vanelli-Coralli, *Senior Member, IEEE*, and Maria Rita Palattella, *Member, IEEE*

***Abstract*— Through the transition from 5G to 6G, a significant rise in the number of Internet of Things (IoT) devices is anticipated, enabling pervasive and uninterrupted connectivity for several applications, in different verticals. Coping with the substantial influx of IoT devices and fulfilling the high capacity demands of different IoT technologies, such as NB-IoT, will necessitate the involvement of Non-Terrestrial Networks (NTNs), which will serve as crucial complements to terrestrial systems, enhancing the availability, resilience, and coverage of the network and will guarantee cost/benefit for some services and will fully satisfy some key requirements. Nevertheless, a primary obstacle to be faced when integrating IoT terrestrial communication systems in NTN, in particular with Non-Geostationary satellites, lies in the short visibility time of the flying platform due to its high speed. The latter introduces criticalities in various communication phases, including the Random Access (RA) procedure. In a highly congested scenario, the large Round Trip Delay and a limited visibility window, which varies for each user within the satellite's coverage area, contribute to reducing the number of users successfully concluding the RA procedure. In this paper, to enhance the percentage of users who successfully conclude the RA, we introduce the concept of Coverage Enhancement Levels in time and a novel backoff mechanism, namely Smart Backoff, that leverages the beam coverage visibility period of individual users to adjust the random backoff interval. The numerical results obtained from our proposed scheme substantiate significant improvements compared to the standard backoff scheme. Specifically, our approach yields an increase of up to 16% per channel in the percentage of users who successfully complete the RA process.**

***Index Terms*— NB-IoT, NTN, random access, backoff.**

I. Introduction

THE integration of Non-Terrestrial Networks (NTN), consisting of satellites and High Altitudes Platform Systems (HAPS), into New Radio (NR), has been one of the critical directions explored in the Third-Generation Partnership Project (3GPP) [1], [2]. The NR was designed for forward compatibility, support for low latency, advanced antenna technologies, and spectrum flexibility including operation in low, mid, and high-frequency bands. In addition to NR protocols, there are also ongoing efforts to integrate the Narrowband Internet of Things (NB-IoT) in NTN [3]. In the current standard, *i.e.*, Rel.17, Geostationary Earth Orbit (GEO), Medium Earth Orbit (MEO), Low Earth Orbit (LEO), and HAPS are supported. In this context, one of the most beneficial and challenging scenarios is adopting LEO satellites as an NTN platform. Indeed, low orbits are characterized by reduced latency (comparable to the terrestrial one in the case of very LEO (vLEO)) and offer an improved link budget compared to GEO or MEO. However, due to the satellite's motion, several issues need to be faced, *e.g.*, high Doppler shift and limited visibility time per satellite. In order to overcome them, one promising solution, that has become a baseline for NB-IoT over NTN within the 3GPP community [3], consists of the use of the Global Navigation Satellite System (GNSS) receiver embedded into the User Equipment (UE). In this way, the UE may use its GNSS location information in combination with satellite ephemeris data to support mobility, compensate for Doppler effects and the large delays, and achieve time and frequency synchronization. A similar approach has been adopted in literature also for no-3GPP LPWAN technologies over NTN, such as satellite LoRaWAN [4].

However, until now, there has been insufficient emphasis on optimizing network access in congested scenarios, especially considering the limited visibility time of the LEO satellites. The broad coverage of the satellite beam, generally provided by an incomplete constellation in the IoT scenario [5], [6], [7], [8], leads to congestion in the case a large number of users will contend for the limited time/frequency resources defined by the NB-IoT standard, as many market forecasts are predicting. Moreover, when considering a procedure such as Random Access (RA), characterized by a long signaling phase, the congestion can severely impair protocol and system performance, potentially resulting in service unavailability by drastically reducing the percentage of users successfully completing the RA procedure.

In this framework, under the assumption of an uncompleted LEO constellation, we propose two methods to mitigate congestion, aiming at increasing the number of users connected to the network: i) the division of the satellite's coverage area into distinct Coverage enhancement Levels (CLs), where depending on the visibility time, some users are not allowed

Manuscript received 30 July 2023; revised 15 November 2023; accepted 15 December 2023. Date of publication 15 February 2024; date of current version 9 May 2024. This work was supported by the Satellite Network of Experts (SatNEx) V Work Item (WI) 2.8: Innovative Techniques and Technologies for Non-Terrestrial Networks (ONION) Project, funded by European Space Agency (ESA). *(Corresponding author: Carla Amatetti.)*

Carla Amatetti and Alessandro Vanelli-Coralli are with the Department of Electrical, Electronic, and Information Engineering, University of Bologna, 40136 Bologna, Italy (e-mail: carla.amatetti2@unibo.it; alessandro.vanelli@unibo.it).

Madyan Alsenwi and Houcine Chougrani are with the Interdisciplinary Centre for Security, Reliability and Trust, University of Luxembourg, 1855 Luxembourg City, Luxembourg (e-mail: madyan.alsenwi@uni.lu; houcine.chougrani@uni.lu).

Maria Rita Palattella is with the Luxembourg Institute of Science and Technology (LIST), 4362 Esch-sur-Alzette, Luxembourg (e-mail: mariarita.palattella@list.lu).

Color versions of one or more figures in this article are available at https://doi.org/10.1109/JSAC.2024.3365868.

Digital Object Identifier 10.1109/JSAC.2024.3365868

to perform the RA; and ii) the design of a smart Backoff (BO) mechanism that, while being compliant with the NB-IoT standard, provides different BO intervals leveraging the visibility period of UEs to increase the number of users successfully completing the procedure.

A. State of the Art

Following the introduction of the study Item of IoT via NTN in Rel. 17 [9], several scientific publications addressed the adaptation of the terrestrial air interface to the NTN impairments both at the physical (PHY) and Medium Access Control (MAC) layers. Most of the works aimed at mitigating challenges posed by high Doppler, large Round Trip Delay (RTD), and considerable path losses [10], [11], [12], [13], [14].

Nevertheless, the development of the NB-IoT via NTN necessitates not only adapting the air interface to accommodate these NTN peculiarities but also fulfilling the terrestrial standard's prerequisites, including massive connectivity and low power consumption. Consequently, recent studies have primarily concentrated on system-level analyses to address these challenges [15], [16], [17], [18]. In [15] the authors aimed at computing the access probability and the average access time of the NB-IoT RA procedure, considering different satellite scenarios defined by the 3GPP in the TR 36.763 [3], with priority to LEO satellites. Several configurable access parameters typical of the NB-IoT standard such as the BO values, the number of sub-carriers reserved for the preamble transmission, and the periodicity of the RA, and finally, different values of the user density were considered in the performance analysis. The authors observed that by fixing the number of available preambles, both the periodicity and the BO values have a great influence on the performance of the RA. Indeed, the short visibility window of the satellite poses an upper bound to the number of RA Occasion (RAO) and the maximum value of the BO.

In [16], the authors addressed the design of NB-IoT over satellite service, compliant with the 3GPP specifications, in the challenging context of a real application scenario. With the aim of offering a real smart agriculture service operating in Europe, they proposed the adoption of 24 LEO satellites, grouped into 8 different orbits, moving at an altitude of 500 km. The configured protocol stack supports the transmission of tens of bytes generated at the application layer by counteracting the issues introduced by the satellite link through the GNSS receiver. The authors tested both the legacy 4-step RA followed by the data transmission and the Early Data Transmission (EDT) and showed that the latter reduces the communication latency up to 40%. In terms of congestion management techniques for the RA phase, a fixed BO window equal to 65536 ms was considered. Finally, the authors observed that with a reduced number of satellites per orbit (from 3 to 2) is still possible to collect all the generated IoT data, but at the expense of a much higher average communication latency.

A similar approach was followed in [17], where the end-to-end (E2E) packet delay is measured by varying the number of considered cubesats (*i.e.*, 4 or 8). Regarding the RA procedure, the number of preambles is set to 48, the periodicity is fixed to 240 ms, and the BO parameter is 2048 ms, in order to mitigate the probability of collisions. The E2E packet delay is computed by considering the influence of cell selection, the length of the RA procedure, the scheduling decisions, and the actual physical transmission. From their analyses, the authors concluded that the number of satellites within the constellation significantly affects the E2E packet delays. Besides, the time required to complete the RA procedure increases as the number of NTN terminals increases. When more users perform the random access procedure, the number of collisions increases and packet delays also increase.

In [18], the performance of the IoT LEO NTN utilizing LTE-M is evaluated in terms of connection density, which corresponds to the number of users allowing an outage rate of 1%. The latter defines the fraction of the total number of users that fail to deliver their packets to the destination receiver within a transmission delay of at most 10 s. The evaluation results showed that a single LEO satellite can support a connection density of 364 devices per km^2 at 600 km of altitude and 78 devices per km^2 at 1200 km.

B. Paper Contributions

As highlighted in the review of the state of the art, even if the issue of congestion has garnered attention over the last years, no algorithm has been proposed to effectively address it while taking into account the limited visibility window of LEO satellites. In order to cope with such an issue, and, therefore, to increase the number of users who successfully conclude the RA procedure, we propose a novel twofold approach, consisting of the following procedures:

- First, we divide the satellite's coverage area into Coverage enhancement Levels, where a different number of preambles is assigned. The CLs are distinguished by a threshold. The latter is computed by taking into account the visibility time of each user and the length of the transmission (random access and uplink data transmission).
- Second, we enhance the standard backoff[1] mechanism, proposing a smart backoff algorithm. The latter, performed at the UE side, calculates the lower and the upper bound of the BO interval considering the visibility period of each UE and the BO value broadcasted by the gNB. Then, the user randomly selects its BO value in the new customized interval.

In order to implement the two aforementioned techniques, we propose an algorithm to determine the visibility time function of LEO satellites given the locations of the different UEs.

The rest of the paper is organized as follows: in Section II the system architecture is described, Section III provides the problem statement; Section IV details the proposed techniques to mitigate the congestion; in Section V the numerical results are reported, and finally, Section VI concludes the work.

[1]In the current work, following the 3GPP terminology, and the NB-IoT standard, we refer to the backoff as a time parameter, indicating the time delay between a RAO and the next RAO.

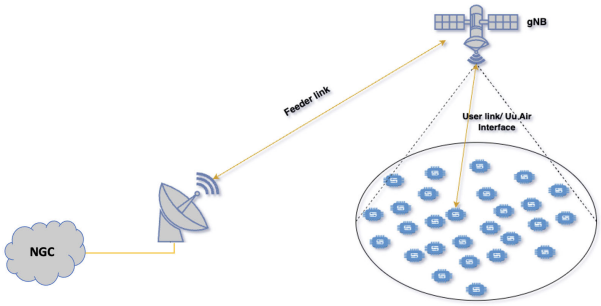

Fig. 1. NB-IoT NTN System architecture with regenerative payload.

TABLE I
SATELLITE PARAMETERS

Satellite orbit	Set 4 LEO 600 km
Equivalent satellite antenna aperture	0.097 m
Sat EIRP density	21.45 dBW/MHz
Sat Tx max Gain	11 dBi
3dB beamwidth	104.7 degree
Sat beam diameter	1700 km
G/T	-18.6 dBK^{-1}
Sat Rx max Gain	11 dBi
Central beam edge elevation	30°
Beam visibility window = $T_{beam} = T_{max}$	246.9 s

II. SYSTEM ARCHITECTURE OF NB-IOT VIA NTN

In the present work, we consider an integrated NTN-NB-IoT network. Hereafter we describe the main elements of the high-level system architecture, according to [1], also illustrated in Fig. 1.

A. The Ground Segment

it comprises N on-ground gateways (GWs) that provide NTN access to the Terrestrial Network(s) (TNs). Specifically, the N GWs establish connectivity between satellites within the constellation, the gNBs, and the Next Generation Core (NGC) network. The configuration of this segment depends on the type of payload on board the NTN elements: i) for transparent payloads, the complete gNB is on the ground, therefore the feeder link, *i.e.*, the link between the GW and the satellite, carries the Uu air-interface; ii) for regenerative payloads the full gNB (shown in Fig. 1) or part of it (if the gNB split is considered) is on-board. With the full gNB on-board, the feeder link transports the NG (Next generation) air interface to interconnect the gNB and the NGC. If the gNB is split into Central Unit (generally on-ground as per 3GPP specifications [20]) and Distributed Unit (on-board the satellite), the feeder link carries the F1 air interface.

B. The Non-Terrestrial Access Segment

It includes the NTN nodes in the constellation. As previously mentioned, the node can host a transparent payload, which basically acts as a rely, or a regenerative payload. In the latter case, depending on whether the functional split is implemented or not, the full gNB or part of it is embarked. Both with the transparent or regenerative payload, the user access link between the satellite and the on-ground UEs is implemented through the traditional Uu air interface. Inter-Satellite Links (ISL) can be employed for the regenerative payload to guarantee a connection between the gNB and the NGC (at the gateway), in case not all the satellites can establish a feeder link. In terms of coverage, the satellite can serve a portion of the on-ground coverage area by means of a single-beam or multi-beam antenna. Moreover, the satellite can be equipped so as to be able to steer the on board antenna in order to always cover the same on-ground area, meaning that the on-ground beams are fixed. On the other hand, the area covered by each satellite will move accordingly with the satellite's movement along its orbit, *i.e.*, the on-ground beams are moving with the satellite since the coverage centre is always located at the sub-satellite point. This second case refers to the so-called moving beams.

C. User Segment

It is represented by a plethora of NB-IoT devices spread all over the world. It is worth noting that, in the case of a sparse constellation, the devices do not have visibility of the satellites for the entire time. The communication capability of the UEs within a specific on-ground coverage area is contingent on the satellite's position along its orbit, allowing only a subset of terminals to establish communication with the flying platform at any given time.

In this paper, the following assumptions for the system configuration hold: i) direct access, *i.e.*, the UE is directly connected to the satellite; ii) a single LEO satellite generating a moving beam, operating in S-band, and equipped with a regenerative payload with the full gNB on-board. This allows to conclude procedures on-boards, *e.g.*, the RA procedure, thus, reducing the impacts of the RTD on the procedure. The satellite configuration is Set 4 according to the nomenclature of TR. 36.763 [3]. In this technical report, the 3GPP has defined four configuration sets that include beam layout, satellite altitude, and Radio Frequency (RF) parameters, namely: Set 1, Set 2, Set 3, and Set 4. The latter defines the largest beam, with the lowest elevation angle (the parameters are shown in Table I). The choice of this large beam is twofold: on the one hand, since only one beam can be generated in the Field of View (FoV) of the satellite, the issue of inter-beam mobility is alleviated, as the mobility is not yet supported for NB-IoT. Moreover, this large dimension ensures a beam coverage time of approximately 4 minutes. Smaller beams would reduce this time. On the other hand, it represents the case where network congestion is highly probable, thus it is an interesting case study. iii) Stationary NB-IoT devices equipped with a GNSS receiver to pre-compensate the Doppler shift and the propagation delay due to the satellite distance.

III. PROBLEM STATEMENT

According to the NB-IoT standard [21], when a UE wishes to connect to the network, it must undergo a process known as Random Access Procedure. Like the legacy Long Term Evolution (LTE) system, this procedure entails the exchange of four messages between the UE and the gNB. These messages

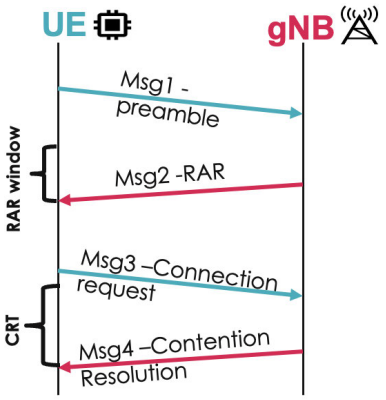

Fig. 2. 4-Steps CBRA.

consist of a preamble (Msg 1), the Random Access Response (RAR or Msg 2), and two Radio Resource Control messages (Msg 3 and Msg 4), as depicted in Fig. 2.

Notably, the most crucial aspect is the preamble transmission, where numerous users contend for the same resources. Indeed, if multiple devices select the same preamble, a collision occurs. The preamble transmission takes place over a spectrum section of 180 kHz, which is divided into 48 or 144 sub-carriers, each with a width of 3.75 kHz or 1.25 kHz depending on the preamble format [22]. This means that a maximum of 48 or 144 preambles are available in each RAO.

In the event of a collision, all UEs that transmitted the same preamble will receive an identical RAR. This is because the decoding key for the RAR relies on the first sub-carrier of the preamble. The RAR message provides both the BO value and the allocated resources for transmitting Msg3. Consequently, the UEs involved in the collision will send their Msg3 on the same time and frequency resources. Ultimately, only one UE will win the contention phase. As a result, UEs who do not receive Msg4, *i.e.*, the contention resolution message, within a time interval namely Contention Resolution Time (CRT), will randomly select a backoff value from the interval $[0, BO]$ [21].

Potentially, each collided terminal has the capability to transmit its preamble in the subsequent RAOs. Defined a time interval, T_{max}, the maximum number of RAOs is given as follow [15]:

$$N_{RAO} = \left\lfloor \frac{T_{max}}{N_{period}} \right\rfloor \tag{1}$$

where N_{period} represents the periodicity of the RAO. In order to mitigate the congestion, a backoff mechanism is introduced. The latter spreads out the activity of the competing devices over time. When multiple UEs collide in an RAO, they will select a backoff value within the range $[0, BO]$ in a random manner. Consequently, the probability that a collided NB-IoT terminal transmits in the $k-th$ RAO, given that it collided in the $n-th$ one, can be calculated as follows:

$$P_{BO} = \begin{cases} \frac{N_{period}}{BO} & \text{if } n + \lfloor \frac{BO}{N_{period}} \rfloor \leq k \\ 0 & \text{if } n + \lfloor \frac{BO}{N_{period}} \rfloor > k \end{cases} \tag{2}$$

The large RTD typical of the NTN influences the choice of the periodicity. Indeed, the periodicity should be long enough to absorb the duration of the RA procedure, given by the length of all the messages represented in Fig. 2, plus two times the RTD [15]. Moreover, in the context of the NTN scenario, the value of T_{max} is contingent on the satellite's coverage area, and it is not the same across all terminals within the satellite's footprint. Consequently, each user has a distinct number of RAOs, which significantly influences the selection of the BO value. The latter holds considerable implications for the performance of the RA procedure, particularly in NTN. Indeed, a small BO value shortens the time interval for devices to re-transmit the preamble, leading to a higher probability of collisions during burst arrivals. Conversely, a large BO value increases the probability of successful access attempts per RAO but may prolong the overall access time, potentially preventing some terminals from re-transmitting if the extracted BO value falls outside their coverage window.

IV. Proposed Solution

In this paper, we propose two techniques to increase the percentage of users successfully concluding the RA procedure during the limited LEO satellite coverage time, described hereafter.

A. Coverage Enhancement Levels in Time

In the terrestrial system, the gNB coverage area is divided into Coverage Enhancement levels (CE) which are defined by power thresholds, according to the requirements of the network [21]. These thresholds are based on the values of the Reference Signal Received Power (RSRP) broadcasted by the gNB. Thus, the UE measures and compares the strength of the received signal with these thresholds. Please note that, as per standard specification, a maximum of three CEs can be defined. The RA parameters dedicated to each CE level can assume different values, which means that each UE applies a different configuration for RA transmissions according to its CE level (*e.g.*, different number of repetitions, frequency location, etc.). In the context of NTN, especially in Line of Sight (LoS) conditions, it is hard to differentiate CE levels by means of power since all UEs have approximately the same radio conditions.

Therefore, our proposal involves partitioning the satellite's coverage area into distinct zones, called Coverage enhancement Levels in time. The idea behind these CLs is to classify the UEs depending on their visibility time within the satellite coverage.

Referring to Fig. 3, we assume that the coverage area is divided into two CLs, one for the UEs that should not transmit their preamble (CL2 in Fig. 3) and the second one where UEs are able to send their preamble (CL1 in Fig. 3). The CLs are defined through a threshold (red line in Fig. 3) and their area depends on the beam dimension.

1) CL1-to-CL2 Threshold Calculation: In order to distinguish the two CL zones, we need to define a CL1-to-CL2 threshold. The latter is mainly a function of the time needed to perform the RA procedure and the data transmission. To establish this threshold, it is necessary to conduct a thorough

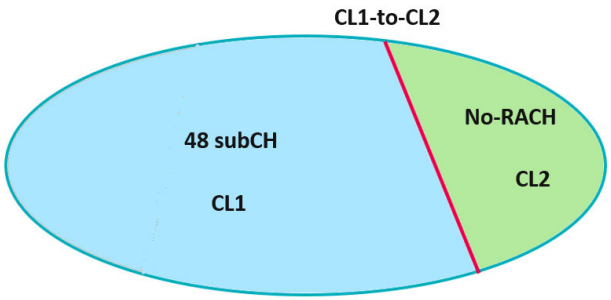

Fig. 3. Illustration of the proposed CL partitions: 2 CLs, and 1 threshold CL1-to-CL2.

evaluation of the suitable time budget required for the message flow in NB-IoT over NTN. Authors in [23] and [24] estimated the transmission time (RA plus data transmission) of the NB-IoT protocol in terrestrial networks and found that it depends on the coupling loss that defines the CE to which the UE belongs. Note that in the terrestrial NB-IoT system, three coupling losses exist [25], which are 144 dB, 154 dB, and 164 dB. UEs with a coupling loss of 144 dB have a good Signal-to-Noise Ratio (SNR), while UEs with 164 dB coupling loss have the worst SNR conditions among the three CEs. It is worth emphasizing that high coupling loss implies a high number of repetitions in both the uplink and downlink as per 3GPP specifications [26], which extends the transmission time. According to [23], the transmission time is $\approx$ 10 seconds for UEs with 164 dB coupling loss, while authors in [24] estimated the transmission time to be $\approx$ 8 seconds for the same coupling loss value. Note that these values are estimated for TNs where the maximum RTD does not exceed 800 μs (*i.e.*, 120 km cell radius). In contrast, for NTN, the RTD values range from $\approx$ 4 ms (resp. $\approx$ 8 ms) to $\approx$ 13 ms (resp. $\approx$ 26 ms) for a regenerative (resp. transparent) LEO satellite at 600 km and are no longer neglected in the transmission time estimation. Since UEs in satellite coverage will have low SNR (estimated to be -12 dB in downlink [3] for Set-4 configuration), a coupling loss of $\approx$ 164 dB is assumed. Accordingly, our methodology is to consider the worst-case scenario in terms of transmission time value in the TN (*i.e.*, the estimated value from [23]) for a coupling loss of 164 dB, and to add 1 second to account for the higher NTN RTD as well as considering a safe margin. Hence, the CL1-to-CL2 threshold is set to 11 seconds.

B. Smart Backoff

While dividing the coverage area of the gNB into different CLs can help in mitigating channel access collisions, there is still a probability that UEs within the same CL will attempt the RA at the same time. The current NB-IoT standard employs a random backoff mechanism to mitigate channel access collisions. However, this mechanism works when all the UEs have the same time to perform the RA. To address this issue, we propose a new backoff mechanism that enables UEs to adjust their backoff interval based on their coverage time. In the standard random backoff approach, each UE chooses a random backoff value from a fixed given interval $[0, \ldots, BO]$, where BO is the upper bound sent by the gNB.

Unlike the classical backoff method, the proposed algorithm allows each UE to adjust its backoff interval considering its coverage time and transmission time in addition to the BO value sent by the gNB that captures network traffic status. Thus, each UE may get a different random backoff interval based on its location in the coverage area, which reduces the collision rate and ensures that both the next channel request attempt and the associated data transmission time fit within the visibility window of the satellite, enhancing the network performance. Therefore, the smart BO algorithm, as the classical BO, aims at distributing the collided users over time, but it improves over the standard mechanism by customizing the backoff interval for each UE and avoids users extracting a BO value which prevents their re-transmission. However, the selection of the backoff time within the obtained backoff intervals is still random; thus, there remains a chance of collisions within the overlapping intervals, particularly among UEs within the same CLs.

1) Upper Bound of the BackOff Interval: Each UE computes the upper bound of the backoff interval using the following equation:

$$\beta^{u}_{\max} = \min\left\{BO, T_{v,u} - T_{tr}\right\}, \forall u \in \mathcal{U}, \tag{3}$$

where U is the set of all UEs in the satellite coverage, T_{tr} is the transmission time, *i.e.*, the sum of RA procedure and data transmission, and $T_{v,u}$ is the visibility time of $u-th$ UE. Eq. (3) allows each UE to decide its upper limit considering the coverage visibility time. Specifically, it ensures that the maximum random backoff waiting time and the transmission time are less than the visibility time so that UE can finalize the transmission process within the satellite visibility time. We can notice that UEs with short visibility time will get smaller backoff intervals than those with longer visibility time.

2) Lower Bound of the Backoff Interval: The proposed smart backoff algorithm adjusts the lower bound of the backoff interval to a desired value instead of setting it to zero like in the classical backoff approach. The objective is to obtain the lower bound of the backoff interval considering the network density and the visibility time of each UE. Specifically, UEs with high visibility time will get a higher value than those with short visibility time. This will force UEs with a long visibility time to get a higher random backoff value as they have enough time to send their data after the backoff delay, giving more transmission opportunities to UEs with short visibility time. Accordingly, each UE can obtain its lower bound of the backoff interval as follows:

$$\beta^{u}_{\min} = \max\left\{0, \beta^{u}_{\max} - \gamma \times N_{\text{period}}\right\}, \quad \forall u \in \mathcal{U}, \tag{4}$$

where γ is a parameter to control the number of transmission opportunities within the selected backoff interval and N_{period} is the periodicity time of random access opportunities. The inclusion of the term $\gamma \times N_{\text{period}}$ guarantees the presence of transmission opportunities within the selected backoff interval. Note that $\beta_{\min}$ is obtained based on the value of $\beta_{\max}$, which depends on visibility time and maximum backoff value broadcasted by the gNB (*i.e.*, BO) according to Eq. (3). Furthermore, the gNB determines the value of BO based on the prevailing network traffic status, *i.e.*, in the case of

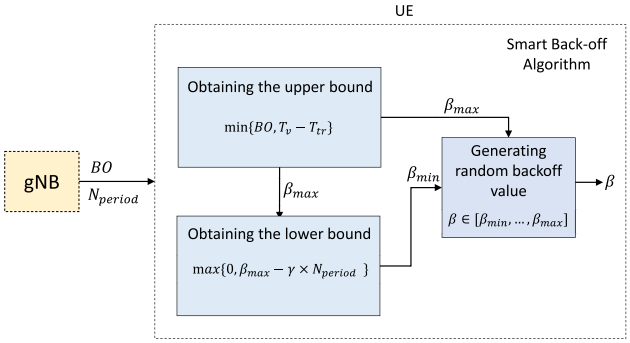

Fig. 4. The proposed smart backoff framework.

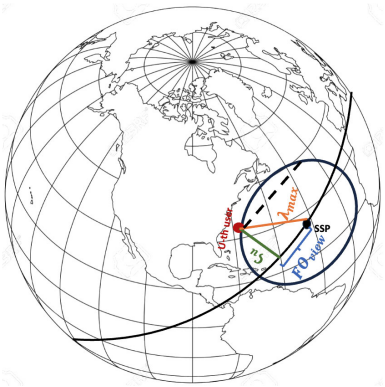

Fig. 5. Earth coverage geometry to compute the maximum visibility period.

high traffic congestion, larger values of BO are selected. This links the lower bound value obtained by Eq. (4) to the network traffic status. Precisely, under circumstances of high traffic congestion, UEs with longer visibility time will get higher values of $\beta_{\min}$ than those with short coverage duration, distributing channel access attempts among UEs based on their coverage visibility time and hence reducing traffic congestion. Conversely, when network traffic is light, the gNB selects a lower value for BO, enabling UEs to select smaller values of $\beta_{\min}$ according to Eq. (3) and Eq. (4) and transmitting their data without incurring undue delays.

Fig. 4 shows the block diagram of the proposed smart backoff framework. In the designed mechanism, each UE first obtains the value of $\beta_{\max}$ based on the received information from the gNB, including BO and the periodicity, and the knowledge of the transmission time T_{tr} and its own satellite coverage time. Then, the value of $\beta_{\min}$ is calculated based on the obtained $\beta_{\max}$, N_{period}, and the value of γ. Finally, the UE randomly selects the actual backoff value from the interval $[\beta_{\min}, \beta_{\max}]$ following the uniform distribution.

C. Computation of the Visibility Time

As mentioned in the previous section, the proposed techniques are based on the knowledge of the UE's visibility time within the satellite coverage.

It is possible to define three angles to characterize the relative position of the UE with respect to the satellite. These three angles are the nadir angle, η_u, measured at the spacecraft from the Sub-Satellite Point (SSP) to the UE; the Earth central angle, λ_u, measured at the center of the Earth from the SSP to the UE; and, finally, the elevation angle, ε_u, measured at the UE between the spacecraft and the local horizontal. Considering moving beams, these angles are symmetric w.r.t the SSP. In both the half of the beams, the domain of the elevation angle ε_u is $[0, \pi/2]$, where $\varepsilon_u = 0$ means that the satellite is at the horizon and $\varepsilon_u = \pi/2$ implies that it is at the Nadir. Accordingly, $\lambda_u \in [\lambda_h, 0]$ and $\eta \in [\eta_h, 0]$ for $\varepsilon_u \in [0, \pi/2]$, where λ_h and η_h are the maximum Earth central angle and nadir angle when the satellite is at the horizon. By imposing a certain beamwidth of the satellite, the coverage area is identified by a minimum elevation angle ε_{min}, a maximum Earth central angle λ_{max}, and a maximum Nadir angle η_{max}. This assumption limits the domains of the angles in the following way: $\varepsilon_u \in [\varepsilon_{min}, \pi/2]$, $\lambda_u \in [\lambda_{max}, 0]$, $\eta_{max} \in [\eta_u, 0]$.

The UE knows these angles as well as the ephemeris of the satellite and it is equipped by the GNSS. The terminal can communicate with the satellite if $\lambda_u \leq \lambda_{max}$ or equivalently $\varepsilon_u \geq \varepsilon_{min}$.

Our objective is to calculate the time during which a specific UE in the beam remains within the satellite coverage area. Considering a satellite on a circular orbit at an altitude H (in km), the orbit Period P in minutes is obtained as follows:

$$P = 2\pi \sqrt{\frac{(R_e + H)^3}{M_e \cdot G \cdot \frac{60^2}{1000^3}}} \tag{5}$$

where R_e is the Earth radius, $M_e = 5.9722 \cdot 10^{24}\ kg$ is mass of the Earth, and $G = 6.674 \cdot 10^{-11}\ m^3/(kg \cdot s^2)$ is the gravitational constant. In this framework, the maximum Earth central angle represents the radius of the access area relevant to the specific observation. This radius, when doubled, is referred to as the "swath width," denoting the width of the coverage path across the Earth's surface. The coverage associated with any $u-th$ user on the Earth's surface is determined by two factors: λ_{max}, and the off-track angle denoted ζ_u, which identifies the perpendicular distance from $u-th$ user to the ground track of the satellite for the orbital pass under examination. Therefore, the Fraction of the Orbit (FO) over which the $u-th$ user is in view (illustrated in Fig. 5) is computed as follows [27]:

$$FO_{view,u} = \frac{1}{180} \cos^{-1}\left(\frac{\cos\lambda_{max}}{\cos\zeta_u}\right) \tag{6}$$

Thus, the time in view is:

$$T_{v,u_{max}} = P \cdot FO_{view,u} = \frac{P}{180} \cos^{-1}\left(\frac{\cos\lambda_{max}}{\cos\zeta_u}\right) \tag{7}$$

Eq. 7 provides the maximum fraction of time over which the $u-th$ UE will be in view considering a full satellite pass over the service area. However, to be able to determine the CL and the BO interval, it is necessary to know the residual visibility window of each UE within the coverage area. In the example provided in Fig. 6, the FO over which the $u-th$ user is in view is in purple.

Let us define the two points on the ground track at the time instant t_a and $t_b = t_a + N_{period}$, which represent two

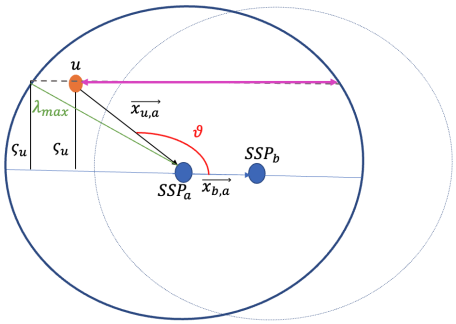

Fig. 6. Geometrical framework to compute the residual visibility period.

consecutive SSPs. It is worth emphasizing that the value of N_{period} is of the order of ms. The vector between the two SSPs in the ECEF coordinates system is given by $\vec{x}_{b,a}$ while the vector from the terminal to the SSP in the current RAO is $\vec{x}_{u,a}$. The angle between the two vectors, illustrated in Fig. 6, is obtained as follows:

$$\vartheta = \cos^{-1}\left(\frac{\vec{x}_{b,a}\vec{x}_{u,a}}{|\vec{x}_{b,a}||\vec{x}_{u,a}|}\right) \tag{8}$$

This angle provides insight into the position of a UE relative to the direction of the satellite's movement. Specifically, when dealing with a moving beam, all three angles mentioned above exhibit symmetry concerning the SSP. Thus, based solely on these angles, it is not possible to understand whether the beam is approaching or moving away from the UEs within the coverage area.

Therefore, exploiting the theorem of the cosine in the spherical geometry, the remaining visibility time for each user is given by, as in (9), shown at the bottom of the next page.

V. Numerical Results

In this section, we provide the outcome of the system-level study performed to evaluate the performance achievable with the proposed methods. The analyses have been performed with a Matlab simulator for the movement of the satellite and the simulation of the RA. Moreover, Matlab has been used to reproduce the Block Error Rate (BLER) curve of the Narrowband Physical Uplink Shared Channel (NPUSCH). In particular, we evaluate the performance in terms of the percentage of users who successfully complete the RA (indicated as *completed users* in Fig. 8a) and the average time to conclude the RA procedure.

As previously mentioned, the satellite coverage region is partitioned into two CLs. It follows that all the preambles, and thus, all the 48 sub-carriers are available for all the users within CL1, as the users in CL2 cannot transmit their preambles. In our model, the beam visibility window defines the upper bound to the number of re-transmissions that a UE can perform to finalize the procedure. Once the RA periodicity is fixed, the maximum number of RAO is computed.

In terms of user density, we considered the following three values $\alpha = [1, 1.5, 2.2] \cdot 10^{-3}[users/km^2/channel]$. Compared to the parameters recommended by 3GPP for terrestrial communication systems, where the user density is 400 $user/km^2$ with an activity factor of 1% [28], it may seem that the NTN system cannot support the traffic density typical of the terrestrial networks. However, it should be noted that in the system we are considering only 1 bearer, *i.e.*, only one channel with 180 kHz bandwidth. Thus, these densities refer to the users per km^2 per channel. It is worth emphasizing that we focus on the optimization of the baseline 180 kHz channel assuming that, once the optimization is achieved for a single channel, the capacity can be scaled up by adopting a larger number of channels, eventually in combination with the frequency reuse.

TABLE II
Access Configuration Parameters

Parameters	Value
N_{period}^{NPRACH}	640ms
Preamble format	1
Number of available preambles	48
Backoff	$[0, 256 \cdot 2^j]$ms, $j \in [0, 11]$
Backoff index	$ID \in [1, 13]$
Uplink repetitions	16

Table I and Table II summarise the satellite parameters and the access parameters, respectively, used when simulating the system and assessing its performance.

A. System Model Implementation

In this work, we considered the model proposed in [15]. Fig. 7 shows the implemented scenario, where an LEO satellite covers an area defined by its FoV and a certain number of UEs, equipped by an omnidirectional antenna, are deployed following a uniform distribution (the blue and colored dots in Fig. 7). The UEs can communicate with the satellite only if they are within the beams. To determine if the user is within the satellite beam, the analysis incorporates the satellite's radiation pattern, a crucial factor also utilized in calculating the link budget. According to the 3GPP specification, the satellite's antenna radiation pattern is defined using a Bessel function. Additionally, for each satellite Set, the 3dB beamwidth angle is specified (for Set 4, this information is presented in Table I). This specification allows for the computation of the radiation pattern at the beam edge, denoted as $\Omega(\eta_{edge})$. Consequently, by evaluating the angle between the satellite's antenna boresight and the direction of the user in the beam, represented as η_u^s, the radiation pattern at the user location, denoted as $\Omega(\eta_u^s)$, can be calculated. If $\Omega(\eta_u^s)$ is higher than $\Omega(\eta_{edge})$, it confirms that the user is inside the beam. $\Omega(\eta_{edge})$ is set to -3dB. Referring to Fig. 7, the colored dots represent all the users who can communicate with the satellite at each step of the simulation, while the red dots are the SSPs at every step of the simulation. The simulation step corresponds to the value of the random access periodicity. Therefore, a new satellite position (SSP) is obtained at each RAO.

The users interfere with each other only if they choose the same preamble. To address the contention arising from multiple collisions, and thus, to define who wins the RA procedure, the Carrier to Interference plus Noise Ratio (CINR) of each UE is utilized to estimate the BLER of the received signal. This

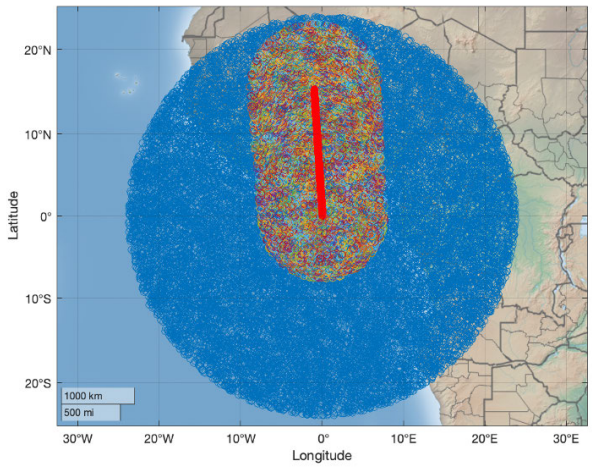

Fig. 7. Simulated region.

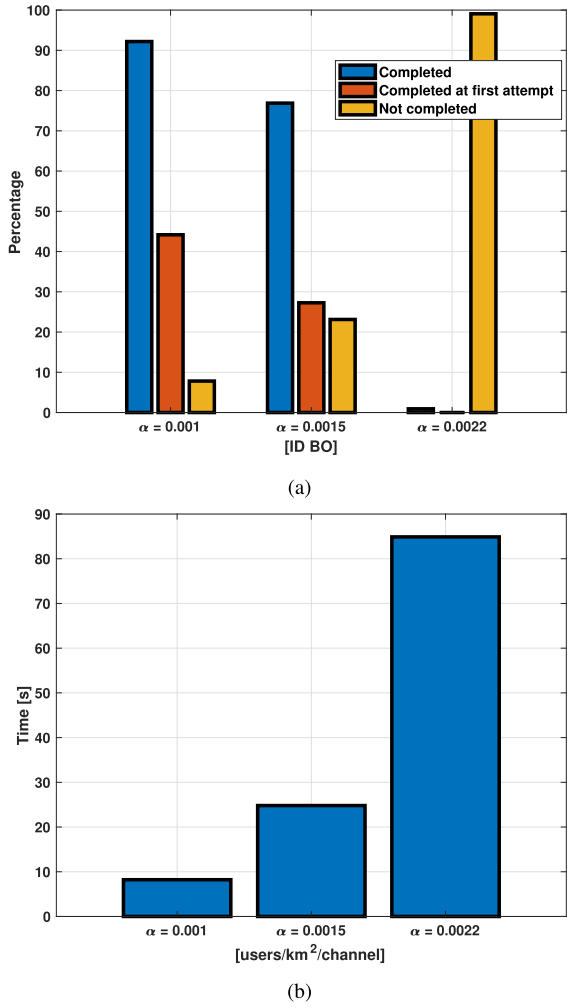

Fig. 8. (a): Analysis of the RA procedure success probability (blue), success probability at the first attempt (orange), and percentage of users who did not conclude the procedure (yellow). (b): Average time to conclude the procedure. Without backoff mechanism.

estimation is performed using CNR-BLER curves specific to the NPUSCH under AWGN (Additive White Gaussian Noise) channel assumption. The model relies on the CNR level of the Msg3 (considering also the repetition of the message), which plays a pivotal role in resolving contentions. Being the first message to contain bits, Msg3 allows for the decoding of transmitted information, making it instrumental in contention resolution. In contrast, Msg1 cannot be used for contention resolution, as it does not carry any information bits, being an unmodulated waveform. In cases where multiple UEs exhibit a CINR exceeding the threshold that provides a BLER of 10^{-1} [29], the UE with the highest CINR is selected. The details to compute the link budget and, therefore, the CINR can be found in [15], [30], and [31].

1) No Backoff and No CLs: To assess the impact of the limited visibility time on the RA procedure when several UEs are competing for channel access at the same time, we first evaluated the performance of the system without implementing the standard backoff mechanism and CLs. Indeed, the objective of this first analysis is to understand the limit of the current NB-IoT NTN system without adopting any countermeasures against the possible congestion in the RA phase. This can be considered as the worst-case scenario of our performance analysis.

Fig. 8a provides the percentage of: i) users who successfully computed the RA (completed), ii) users who successfully computed the RA at their first attempt (completed at first attempt), and iii) users who did not complete the procedure (not completed). The bar graph shows that a greater value of α leads to a higher number of collisions. Such a result was expected. Indeed, since more devices try to send a preamble in the same RAO, the collision probability increases accordingly. As a consequence, the percentage of users who finalize the procedure decreases with the traffic load. Fig. 8a also shows the percentage of users who complete the procedure in their first available RAO. By keeping this percentage high, it is possible to reduce the average time needed to perform the RA procedure. This is confirmed by the results in Fig. 8b. Indeed, the lower the number of collisions, the higher the percentage of users who can complete the procedure on the first attempt, and thus, the shorter the average time to complete the procedure. Moreover, by reducing this time, users have more time for data transmission. It is noteworthy that the percentage of users who successfully finish the RA on their first attempt is a portion of the total percentage of users who have completed the procedure. Indeed, starting from the

$$T_{v,u} = \begin{cases} \left(\frac{P}{360}\right)\left[\cos^{-1}\left(\frac{\cos\lambda_{max}}{\cos\zeta_u}\right) + \cos^{-1}\left(\frac{\cos\lambda_u}{\cos\zeta_u}\right)\right], & \text{if } \vartheta \geq \frac{\pi}{2} \\ \left(\frac{P}{360}\right)\left[\cos^{-1}\left(\frac{\cos\lambda_{max}}{\cos\zeta_u}\right) - \cos^{-1}\left(\frac{\cos\lambda_u}{\cos\zeta_u}\right)\right], & \text{if } \vartheta < \frac{\pi}{2} \end{cases} \tag{9}$$

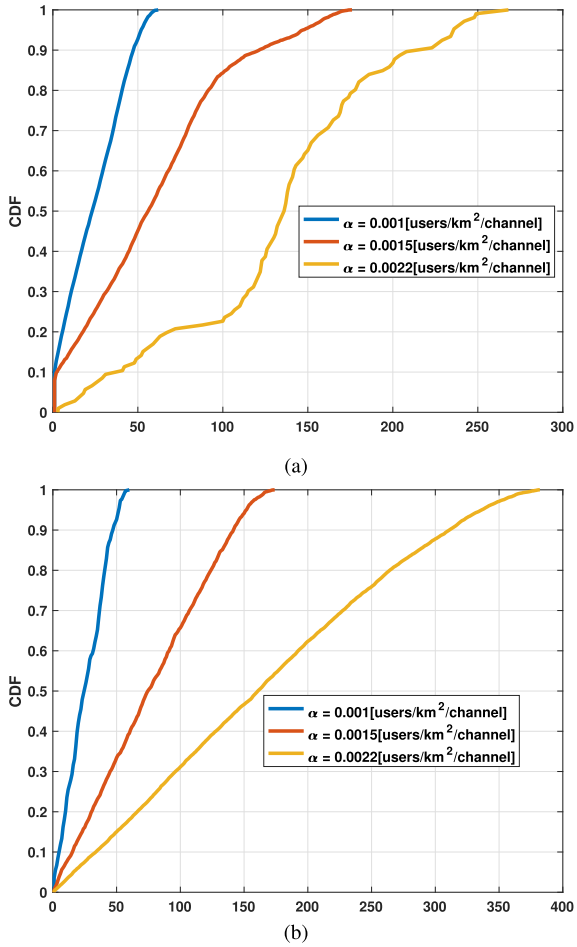

Fig. 9. CDF of the number of attempts of the users who win (a) and fail (b) the RA procedure, without backoff mechanism.

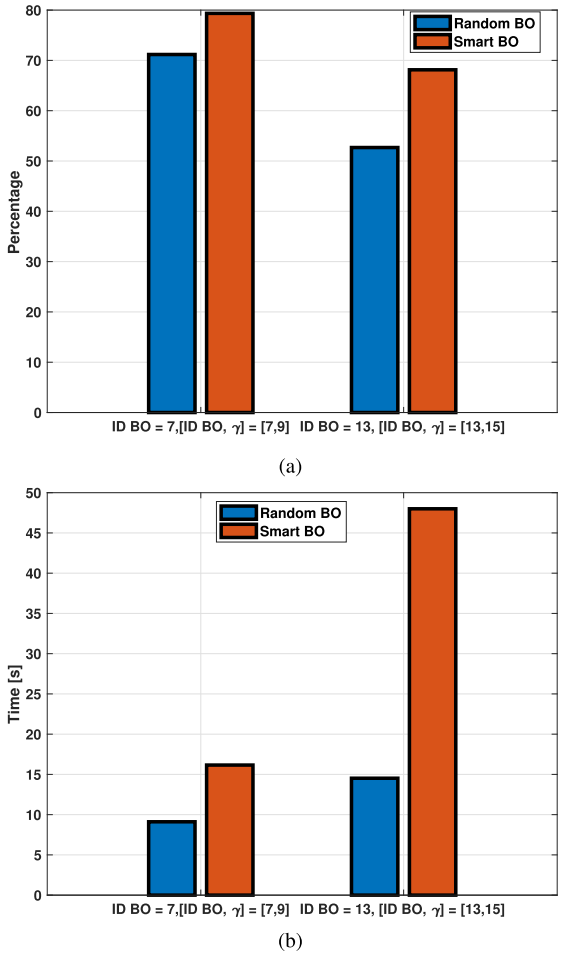

Fig. 10. Percentage of users who successfully conclude the RA (a). Average time to conclude the RA (b). Random vs smart BO. $\alpha = 0.003[users/km^2/channel]$.

first absolute random access occasion of the simulation (*i.e.*, $RAO = 1$) there are always more terminals than the available preambles according to the simulated scenarios. Based on the standard, in the case of collisions, only one user per preamble can win the contention, if there exists at least one user with an SINR bigger than the threshold. Thus, at this moment, the two percentages are equal. However, all users colliding in $RAO = 1$ who will win in other RAOs will contribute to the percentage of users who conclude the procedure. Since the satellite moves, new users will be covered by the beam and they will send the preamble for the first time in a $RAO > 1$. If they successfully conclude the procedure in the same RAO, they will contribute to both the percentage of users who successfully finish the RA on the first attempt and the percentage of users who successfully finish the RA. Otherwise, if they collide and win in another RAO they will be included only in the percentage of users who completed the procedure. Finally, Fig. 9a and Fig. 9b show the Cumulative Distribution Function (CDF) of the number of transmissions used by users who successfully completed the procedure and of the users that failed it, respectively. As expected, the steepest curve is obtained with the lowest α in both cases. While, when the system is saturated (*i.e.*, $\alpha = 0.0022[users/km^2]$), in 90% of the cases, the number of re-transmissions is smaller than 220 and 310, respectively.

2) Random Vs Smart BackOff: Results presented in the previous section demonstrated that the system collapses with user density $\alpha = 0.0022[users/km^2/channel]$, when not implementing any BO mechanism. Therefore, we have further tested the system, first using the standard random backoff and then implementing the proposed smart backoff. In both cases, we considered the threshold CL1-to-CL2 equal to 11 [s] (see Fig. 3).

We decided to set the density to $\alpha = 3 \cdot 10^{-3}[users/km^2/channel]$ to see if there are enhancements with the BO under a more congested scenario.

Fig. 10a compares the success rate of random access obtained with both the random and the smart BO. Two different values of the BO indices (7 and 13) are considered to evaluate the effect of the number of re-transmissions given the limited satellite visibility period.

High BO indices distribute the users in more RA opportunities when implementing the standard random BO. This allows for reducing the probability of collision. However, since the time to perform the RA is bounded by the satellite's visibility period, the total number of attempts within the time window is limited. Furthermore, since users have different visibility periods (between 0 and 4 minutes due to their different positions

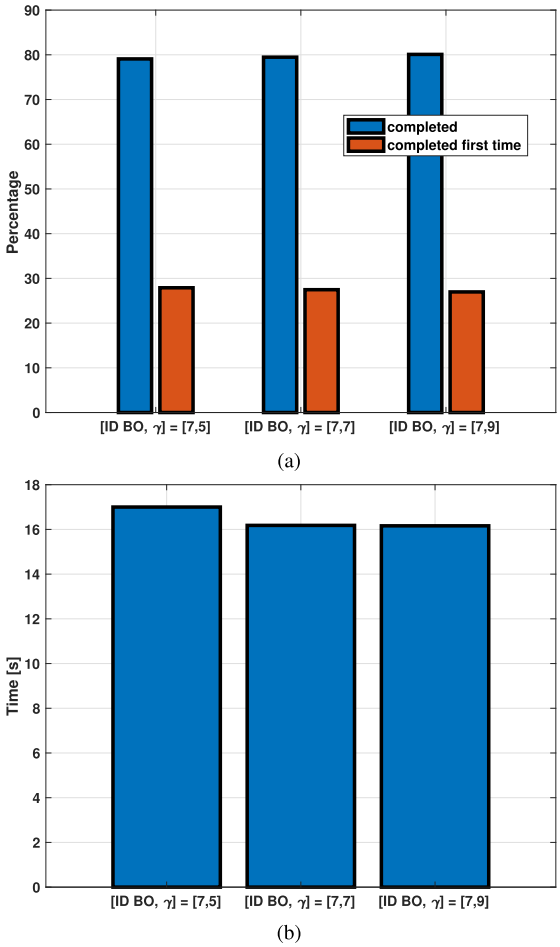

Fig. 11. Percentage of users who successfully the RA procedure (a). Average time to conclude the RA (b). Smart BO index = 7 with different values of γ. $\alpha = 0.003[users/km^2/channel]$.

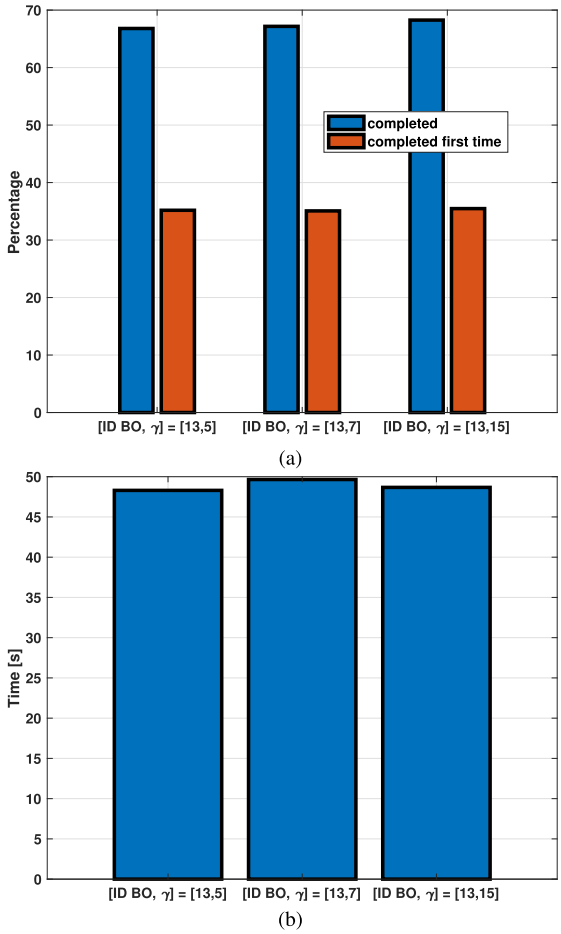

Fig. 12. Percentage of users who successfully computed the RA (a). Average time to conclude the RA (b). Smart BO index = 13 with different values of γ. $\alpha = 0.003[users/km^2/channel]$.

inside the beam), it may happen that, devices randomly extract a BO value that allows them to transmit only when they are outside the satellite's beam. Thus, in the end, they will not be able to send the preamble. This behavior is confirmed in Fig. 10a where the blue bar represents the performance achievable with random BO. When using a BO index equal to 13, the percentage of users able to perform the RA successfully only reaches 52%, due to the fact that users randomly choose a BO value higher than their actual visibility time. BO index equal to 7 provides better results, as the users are uniformly distributed on fewer occasions (*i.e.*, 12). This reduces the number of users who extract a BO value greater than their visibility time.

As previously described, the smart backoff controls the number of random access occasions through γ and it takes into account the visibility time of the users, avoiding that the UEs extract a BO value which can prevent them from re-transmission. These two factors increase the success rate as demonstrated in Fig. 10a.

Indeed, when comparing the results obtained with BO index equal to 13, with both the smart and random backoff, the former provides an increase of 16% in the RA success probability. With the random BO, the users are spread over 819 RA opportunities, while with the smart BO in only 15. With BO index equal to 7, the smart BO increases the percentage of the users winning the access by 10 % as the users are distributed in 9 opportunities provided by the random BO. Moreover, the maximum value of the smart BO takes into account the coverage time. In terms of time to conclude the RA, the smart BO provides higher values than the random one, as visible in Fig. 10b. This is justified by the fact that the reduction of the number of opportunities between the minimum and the maximum BO value leads to an increase in the collision probability, compared to the standard BO mechanism. Thus, the users attempt the access more time. However, the results show that the collisions only impact the time to terminate the procedure, but the overall access rate is higher with the smart BO.

3) γ Optimization: Finally, we tested the performance achievable with the smart backoff when using different values of γ. As explained before, γ impacts the number of random access occasions between the minimum and maximum backoff value. The results in terms of RA success rate and average time to gain the access are presented in Fig. 11a, 11b, 12a and, 12b. In the case of BO ID = 7, higher values of γ produce slightly better results as the users are distributed in more opportunities, and thus, the probability of collision is lower. With $\gamma = 9$, the gain of the percentage of terminals that successfully concluded

the RA is 1.5%, while the average time is reduced by almost one second. Regarding BO ID $= 13$, improvements are visible with $\gamma = 15$, especially in terms of RA success rate (increased of 2.5%). As the BO ID is large, it is possible to consider higher values of γ to better distribute the collided terminals in different opportunities. The value of γ should be properly selected in the system design, to find the best trade-off among the different KPIs. The optimization of γ depends on the user density and its distribution. Through simulations, we found that with this density and the uniform distribution, the value of γ which provides the best results in terms of both delay and percentage of users who successfully conclude the RA is 9 for a BO ID equal to 7, while for BO ID equal to 13, the optimal γ is 15.

B. Considerations on Standardization and UE Impact

The core of the proposed smart backoff algorithm is designed to be implemented on the UE side. This means that the gNB operates within the existing framework, sending BO intervals as per the standard procedures. The innovation lies in how UEs, upon receiving this standard BO information from the gNB, recalculate their backoff intervals by also considering their individual visibility times and the transmission time. So the impact is on the implementation and not on the standard specification. Note that the threshold of the two coverage levels is fixed in this work. However, if one defines a dynamic threshold, an impact on the specification is inevitable. In practice, if the latter is true, the value of this threshold should be communicated to UEs via the downlink control channel.

In NTN configuration, UEs are supposed to use ephemeris information and their location knowledge to predict the future passes of the satellite, Doppler, and propagation delay [3]. The additional step in our method is to calculate the pass duration from geometrical consideration and deduce the upper and lower bounds of the BO value. To this aim, a firmware update on the UE would be necessary for estimating the upper and lower bounds of the BO value, without impacting the complexity of the user.

VI. Conclusion and Future Work

In this paper, we addressed the issue of RA congestion that can occur in NTN NB-IoT networks. To reduce the RA congestion probability, we proposed to divide the coverage zone of the satellite into Coverage Enhancement Levels in time, preventing the transmission of the preamble to the UEs without sufficient time to conclude their RA and the data transmission. Furthermore, in the CL where the preamble transmission is allowed, we proposed a smart backoff mechanism based on the coverage time of each UE and the BO value broadcasted by the gNB.

The simulation results proved that thanks to the proposed RA optimization mechanisms, we can reduce the collision probability during the NB-IoT RA. Therefore, the UEs have more chance to be identified rapidly (via random access) and consequently send their data within the limited visibility time of the LEO satellite. A gain of $10\% - 16\%$ in the RA success probability was obtained, compared to the standard random backoff, used in terrestrial NB-IoT networks.

While in this paper we studied the case with two CLs, in our future work, we will consider three CLs and investigate if in this way the collision probability can be further reduced. Moreover, it is necessary to examine the impact of the distribution of users, which strongly influences the selection of the optimal γ.

Acknowledgment

This work was supported by the Satellite Network of Experts (SatNEx) V Work Item (WI) 2.8: Innovative Tecniques and Technologies for Non-Terrestrial Networks (ONION) project funded by European Space Agency (ESA). The authors would like to thank Dr. Nader Alagha and Dr. Stefano Cioni from ESA for their constructive discussions. The views expressed in this article can in no way be taken to reflect the official opinion of the European Space Agency.

References

[1] *3rd Generation Partnership Project; Technical Specification Group Radio Access Network; Study on New Radio (NR) to Support Non Terrestrial Networks (Release 15)*, document TR 38.811, Version 15.1.0, 3GPP, 2019.

[2] *Solutions for NR to Support Non-Terrestrial Networks (NTN)*, document TR 38.821, Version 16.0.0, 3GPP, 2020.

[3] *Study on Narrow-Band Internet of Things (NB-IoT)/Enhanced Machine Type Communication (eMTC) Support for Non-Terrestrial Networks (NTN) (Release 17)*, document TR 36.763, Version 17.0.0, 3GPP, 2021.

[4] M. Afhamisis and M. R. Palattella, "SALSA: A scheduling algorithm for LoRa to LEO satellites," *IEEE Access*, vol. 10, pp. 11608–11615, 2022.

[5] *GateHouse*. Accessed: Jul. 20, 2023. [Online]. Available: https://gatehousesatcom.com/news/the-worlds-first-5g-narrow-band-iot-satellite-terminal/

[6] *Mediatek*. Accessed: Jul. 20, 2023. [Online]. Available: https://www.mediatek.com/

[7] *Sateliot*. Accessed: Jul. 20, 2023. [Online]. Available: https://sateliot.space

[8] *Successful Launch of Tiger-2 Satellite Aboard Spacex Transporter-2 Mission*. Accessed: Jul. 20, 2023. [Online]. Available: https://www.oqtec.space/news/successful-launch-of-tiger-2-satellite-aboard-spacex-transporter-2-mission

[9] *Study on NB-IoT/eMTC Support for Non-Terrestrial Network*, document RP-193235, MediaTek, 2019.

[10] A. Guidotti et al., "Architectures and key technical challenges for 5G systems incorporating satellites," *IEEE Trans. Veh. Technol.*, vol. 68, no. 3, pp. 2624–2639, Mar. 2019.

[11] G. Charbit, D. Lin, K. Medles, L. Li, and I.-K. Fu, "Space-terrestrial radio network integration for IoT," in *Proc. 2nd 6G Wireless Summit (6G SUMMIT)*, Mar. 2020, pp. 1–5.

[12] M. Conti, S. Andrenacci, N. Maturo, S. Chatzinotas, and A. Vanelli-Coralli, "Doppler impact analysis for NB-IoT and satellite systems integration," in *Proc. IEEE Int. Conf. Commun. (ICC)*, Jun. 2020, pp. 1–7.

[13] M. Conti, A. Guidotti, C. Amatetti, and A. Vanelli-Coralli, "NB-IoT over non-terrestrial networks: Link budget analysis," in *Proc. IEEE Global Commun. Conf.*, Dec. 2020, pp. 1–6.

[14] C. Amatetti, M. Conti, A. Guidotti, and A. Vanelli-Coralli, "Preamble detection in NB-IoT via satellite: A wavelet based approach," in *Proc. IEEE Global Commun. Conf. (GLOBECOM)*, Dec. 2021, pp. 1–6.

[15] C. Amatetti, M. Conti, A. Guidotti, and A. Vanelli-Coralli, "NB-IoT random access procedure via NTN: System level performances," in *Proc. IEEE Int. Conf. Commun.*, May 2022, pp. 2381–2386.

[16] G. Sciddurlo et al., "Looking at NB-IoT over LEO satellite systems: Design and evaluation of a service-oriented solution," *IEEE Internet Things J.*, vol. 9, no. 16, pp. 14952–14964, Aug. 2022.

[17] A. Petrosino, G. Sciddurlo, S. Martiradonna, D. Striccoli, G. Piro, and G. Boggia, "WIP: An open-source tool for evaluating system-level performance of NB-IoT non-terrestrial networks," in *Proc. IEEE 22nd Int. Symp. World Wireless, Mobile Multimedia Netw. (WoWMoM)*, Jun. 2021, pp. 236–239.

[18] J. Sedin et al., "5G massive machine type communication performance in non-terrestrial networks with LEO satellites," in *Proc. IEEE Global Commun. Conf. (GLOBECOM)*, Dec. 2021, pp. 1–6.
[19] *Study on Narrow-Band Internet of Things (NB-IoT)/Enhanced Machine Type Communication (EMTC) Support for Non-Terrestrial Networks (NTN)*, document 36.763, 3GPP, 2021.
[20] *Solutions for NR to Support Non-Terrestrial Networks (NTN)*, document 38.821, Jun. 2021.
[21] *Evolved Universal Terrestrial Radio Access (E-UTRA); Physical Layer Procedures*, document 36.213, 3GPP, Jun. 2021.
[22] H. Chougrani, S. Kisseleff, W. A. Martins, and S. Chatzinotas, "NB-IoT random access for nonterrestrial networks: Preamble detection and uplink synchronization," *IEEE Internet Things J.*, vol. 9, no. 16, pp. 14913–14927, Aug. 2022.
[23] *Latency Evaluation for Guard-Band Operation*, document R1-157250, 3GPP, Nokia Netw., Nov. 2015.
[24] *NB-IoT—Exception Report Latency Evaluation*, document R1-156027, 3GPP, TSG RAN1, Ericsson, ZTE, Alcatel-Lucent, Alcatel-Lucent Shanghai Bell, Nokia, Intel, Samsung, LGE, Oct. 2015.
[25] *3rd Generation Partnership Project; Technical Specification Group Radio Access Network; Study on Provision of Low-cost Machine-Type Communications (MTC) User Equipments (UEs) Based on LTE (Release 12)*, document TR 36.888, Version 12.0.0, 3GPP, 2013.
[26] *36.211—Evolved Universal Terrestrial Radio Access (E-UTRA); Physical Channels and Modulation*, document 36.211, 3GPP, Jun. 2021.
[27] J. R. Wertz, W. J. Larson, D. Kirkpatrick, and D. Klungle, *Space Mission Analysis and Design*, vol. 8. Torrance, CA, USA: Microcosm, 1999.
[28] *3rd Generation Partnership Project; Technical Specification Group Services and System Aspects; Service Requirements for the 5G System; Stage 1 (Release 18)*, document TS 22.261, Version 18.6.1, 3GPP, 2022.
[29] *Evolved Universal Terrestrial Radio Access (E-UTRA); LTE Coverage Enhancements*, document 36.824, 3GPP, 2020.
[30] A. Guidotti, A. Vanelli-Coralli, A. Mengali, and S. Cioni, "Non-terrestrial networks: Link budget analysis," in *Proc. IEEE Int. Conf. Commun. (ICC)*, Jun. 2020, pp. 1–7.
[31] *Link Budget Results for IoT NTN*, document R1-2104573, 3GPP, TSG, RAN, WG 1, May 2021.

Carla Amatetti (Member, IEEE) received the M.Sc. degree in communications and computer network engineering from Politecnico of Torino, Turin, Italy, in 2018, and the Ph.D. degree in electronics, telecommunications, and information technologies engineering from the Digicomm Group, Department of Electrical, Electronic and Information Engineering (DEI), University of Bologna, Bologna, Italy, in 2023. From 2018 to 2019, she was with the Fiat Research Center on activities related to 5G for vehicular applications. Since October 2023, she has been a Junior Assistant Professor with the University of Bologna. During the Ph.D. period, she spent seven months at the University of Luxembourg to carry out research on NB-IoT via NTN. She has worked on different international and national funded initiatives on the integration between terrestrial and non-terrestrial networks. Her research interests include non-terrestrial networks, NB-IoT, 5G, and 6G networks at physical and medium access control layers.

Madyan Alsenwi (Member, IEEE) received the M.Sc. degree in electronics and communications engineering from Cairo University, Giza, Egypt, in 2016, and the Ph.D. degree in computer engineering from Kyung Hee University (KHU), Yongin, South Korea, in 2021. Before joining KHU, he was a Researcher on several research projects funded by the Information Technology Industry Development Agency, Egypt. His research interests include resource management in next-generation wireless networks, ultrareliable low-latency communications, UAV-assisted wireless networks, and machine learning.

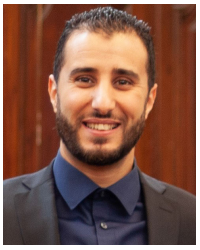

Houcine Chougrani received the State Engineering degree in electronics from École Nationale Polytechnique Algiers, Algeria, in 2011, the M.Sc. degree in signal processing from Paul Sabatier University, Toulouse, France, in 2012, and the Ph.D. degree in information technology from École Telecom Bretagne, Brest, France, in 2016. From 2017 to 2018, he was a Research and Development Engineer with the Department of Telecommunication, Airbus Defence and Space. From 2018 to 2019, he was a Research and Development Engineer with OQ Technology. He is currently a Research Scientist with the SnT, University of Luxembourg. His research interests include the development and implementation of advanced techniques for both terrestrial and satellite communication focusing on the 3GPP-based protocols.

Alessandro Vanelli-Coralli (Senior Member, IEEE) received the Dr.Ing. degree in electronics engineering and the Ph.D. degree in electronics and computer science from the University of Bologna, Bologna, Italy, in 1991 and 1996, respectively. In 1996, he joined the University of Bologna, where he is currently a Full Professor. From 2003 to 2005, he was a Visiting Scientist with Qualcomm Inc., San Diego, CA, USA. He chaired the Ph.D. Board, Electronics, Telecommunications and Information Technologies from 2013 to 2018. He participates in national and international research projects on wireless and satellite communication systems and he has been a project coordinator and scientist responsible for several European Space Agency and European Commission-funded projects. He is currently responsible for the Vision and Research Strategy Task Force of the Networld2020 SatCom Working Group. He is a member of the Editorial Board of the *Interscience Journal on Satellite Communications and Networks* (Wiley) and an Associate Editor of the Editorial Board of *Aerial and Space Networks Frontiers in Space Technologies*. He has served in the organization committees of scientific conferences. He was a co-recipient of several best paper awards and a recipient of the 2019 IEEE Satellite Communications Technical Recognition Award.

Maria Rita Palattella (Member, IEEE) is currently a Senior Researcher with the Environmental Research and Innovation (ERIN) Department, Luxembourg Institute of Science and Technology (LIST). She is leading the work on the design of innovative communication systems and network architectures for different Internet of Things (IoT) applications, including environmental monitoring, precision agriculture, and natural disaster management. She has served as a PI and the project manager for several national and international projects (FNR LORSAT, SMC Lux5GCloud, IoT4WEED, and H2020 HEMS) investigating the use of IoT for smart agriculture applications (e.g., crop supervision and weed control). Currently, she is a coordinator of the Horizon Europe COMMECT project, aiming to extend connectivity in rural and remote areas, by integrating terrestrial (public and private 5G, IoT, etc.) and Non-Terrestrial (NTN), UAVs, satellite networks. She has investigated IoT protocol optimization for NTN, with a focus on LoRa/LoRaWAN scheduling and synchronization in the FNR LORSAT project, and NB-IoT random access procedure in the SatNEX V ONION project. She is currently a coordinator of the SatNEx V INVENTIVE project, studying IoT connectivity via multi-layer NTN encompassing UAVs and LEO Systems. Prior to that, she was a Research Associate with the Interdisciplinary Centre for Security, Reliability and Trust (SnT), University of Luxembourg. She contributed to the design of MAC protocols and energy-efficient scheduling algorithms for Wireless Sensor Networks. She contributed to several EU FP7 and H2020 projects, as WP and task leader, including OUTSMART, IoT6, and F-Interop. She has (co)authored several papers published in well-known, high-impact journals, and international conferences. She sits on the editorial board of the *Transactions on Emerging Telecommunications Technologies*. She was the co-founder and active member of the IETF 6TiSCH WG, and she was selected as a 6TiSCH expert for three ETSI 6TiSCH Plugtests. She has served as a TPC member for several IoT-related conferences and a reviewer for international conferences and journals. She is the Tutorial Co-Chair for ICC2024.

Open Access funding provided by 'Alma Mater Studiorum - Università di Bologna' within the CRUI CARE Agreement